

Accepted for publication in ApJL

**Stellar Masses of Luminous Compact Blue Galaxies at Redshifts  $z = 0.4 - 1.2$** R. Guzmán<sup>1</sup>, G. Östlin<sup>2</sup>, D. Kunth<sup>3</sup>, M.A. Bershady<sup>4</sup>, D.C. Koo<sup>5</sup>, and M.A. Pahre<sup>6</sup>**ABSTRACT**

We present stellar mass measurements for a sample of 36 Luminous Compact Blue Galaxies (LCBGs) at redshifts  $z = 0.4 - 1.2$  in the Flanking Fields around the Hubble Deep Field North. The technique is based on fitting a two-component galaxy population model to multi-broadband photometry. Best-fit models are found to be largely independent on the assumed values for the IMF and the metallicity of the stellar populations, but are sensitive to the amount of extinction and the extinction law adopted. On average, the best-fit model corresponds to a LMC extinction law with  $E(B-V)=0.5$ . Stellar mass estimates, however, are remarkably independent on the final model choice. Using a Salpeter IMF, the derived median stellar mass for this sample is  $5 \times 10^9 M_{\odot}$ , i.e.,  $\sim 2$  times smaller than previous virial mass estimates. Despite uncertainties of a factor 2-3, our results strengthen prior claims that L\* CBGs at intermediate redshifts are, on average, about 10 times less massive than a typical L\* galaxy today.

*Subject headings:* galaxies: starbursts — galaxies: masses, evolution

**1. Introduction**

Luminous Compact Blue Galaxies (LCBGs) refers to a heterogenous class of starburst systems with typical luminosities around  $L^*$  that become very common at intermediate redshifts (Koo et al. 1994, 1995; Guzmán et al. 1996, 1997; Phillips et al. 1997; Mallén-Ornelas et al. 1999; Hammer et al. 2001). LCBGs are particularly interesting for studies of galaxy formation and evolution since

---

<sup>1</sup>Department of Astronomy, University of Florida, Gainesville, FL 326011, USA

<sup>2</sup>Stockholm Observatory, SE - 106 91 Stockholm, Sweden

<sup>3</sup>Institute d’Astrophysique de Paris, 98 bis, Boulevard Arago, F-75014 Paris, France

<sup>4</sup>Department of Astronomy, University of Wisconsin, Madison, 475 North Charter Street, Madison, WI 53706

<sup>5</sup>University of California Observatories/Lick Observatory, Department of Astronomy and Astrophysics, University of California, Santa Cruz, CA 95064

<sup>6</sup>Harvard-Smithsonian Center for Astrophysics, 60 Garden Street, Cambridge, MA 02138

they have evolved more than any other galaxy class in the last  $\sim 8$  Gyrs (Mallén-Ornelas et al. 1999), and have been identified as a major contributor to the observed enhancement of the global star formation rate density of the universe at  $z \leq 1$  (Guzmán et al. 1997; Gruel 2002). Despite their cosmological importance, the nature of LCBGs and their relation to today’s galaxy population still remain largely unknown. The most comprehensive study of LCBGs at intermediate redshift to date –only 45 objects– is that of Phillips et al. (1997) and Guzmán et al. (1997), who concluded that the LCBG class is populated by a mixture of starbursts. About  $\sim 60\%$  of galaxies in their sample are classified as “HII-like” since they are spectroscopically similar to today’s population of vigorously star-forming HII galaxies. The remaining  $\sim 40\%$  are classified as “SB disk-like” since they are more evolved star-forming systems similar to local spirals with a central starburst, and giant irregular galaxies.

Given the diverse nature of the LCBG population, they are unlikely to evolve into one homogeneous galaxy class. There are two popular scenarios. Koo et al. (1994) and Guzmán et al. (1996) have suggested that some subset of the most compact HII-type LCBGs at intermediate redshifts may be the progenitors of local low-mass spheroidal galaxies (or dwarf ellipticals), such as NGC 205. Alternatively, Phillips et al. (1997) and Hammer et al. (2001) have suggested that SB disk-like LCBGs may actually be more massive disks forming from the center outward to become present-day  $L^*$  spirals. At the heart of this debate is the question: are the masses of LCBGs comparable to that of today’s massive or low-mass galaxies? Prior measures of Keck velocity widths and HST sizes show that LCBGs have mass-to-light ratios that are only  $\sim 0.1 - 1.0 M_\odot/L_{B\odot}$ , i.e., about 10 times smaller than a typical  $L^*$  galaxy today (Koo et al. 1994; Guzmán et al. 1996; Phillips et al. 1997). Since ionized gas emission line widths may not reflect the true gravitational potential, an independent estimate of galaxy mass is desirable. Stellar mass is an obvious choice, since HI and CO emission line widths are too difficult to measure in galaxies beyond the local universe.

Several authors have pointed out that the near-IR luminosity of a galaxy is a robust estimator of its stellar mass (e.g., Aragón-Salamanca et al. 1993; Alonso-Herrero et al. 1996; Charlot 1998). The main uncertainty in the inferred stellar masses arises from the age of the stellar population (Rix & Rieke 1993). Instead of using  $H\alpha$  to constrain the strength and age of a young burst (Gil de Paz et al. 2000; Östlin et al. 2001; Pérez-González et al. 2003a, 2003b), an alternative approach when studying galaxies at higher redshifts is to use rest-frame far-UV fluxes (Brinchmann & Ellis 2000, hereafter BE00; Papovich, Dickinson & Ferguson 2001). Here we use a modified version of the method described in BE00 to estimate the stellar masses of a sample of LCBGs at intermediate redshift. Our goal is to test previous claims that LCBGs have, on average, an order of magnitude smaller masses than typical galaxies today with similar luminosities. In section 2 we introduce the photometric data set used in this analysis. Section 3 describes the technique developed to derive stellar masses. The results are summarized in Section 4. For consistency with previous work, throughout this paper we adopt  $H_0 = 50 \text{ km s}^{-1} \text{ Mpc}^{-1}$  and  $q_0 = 0.05$ .

## 2. The Data

The initial galaxy sample consists of 40 LCBGs at redshifts  $0.4 < z < 1.2$  selected from the Flanking Fields around the Hubble Deep Field North, as described in Phillips et al. (1997). A wide variety of information for this sample was made publicly available by the Deep Evolutionary Extragalactic Probe (DEEP) collaboration, including F814W surface photometry, ( $V_{F606W} - F814W$ ) colors, Oxygen and Balmer emission line equivalent widths, velocity widths, star formation rates, and virial masses (Phillips et al. 1997; Guzmán et al. 1997). In addition, deep optical Un, G, R photometry for the entire HDF+FF area is available through the Caltech Faint Galaxy Redshift Survey (Hogg et al. 2000), while deep near-IR photometry in the notched HK' filter is listed in the Hawaii Flanking Field Catalog (Barger et al. 1999). After cross-correlating the various catalogs, we ended up with a final sample of 36 objects with deep Un, G, R, F814W, and HK' photometry. Two thirds of the objects are classified as HII-like, while the remaining one third are classified as SB disk-like. Limiting magnitudes for the photometry in each of these bands are: Un = 25, G = 26, R = 25.5, F814W = 25.0, HK' = 20.7. As described in Phillips et al. (1997), all LCBGs in our sample are brighter than F814W=23.74 mag and their half-light radii are smaller than 0.5 arcsec. For F814W and HK', an estimate of the total magnitude was derived from the total flux within a 3 arcsec diameter aperture. For Un, G, and R, total magnitudes were derived after correcting the magnitudes within 1.7 arcsec diameter apertures for flux outside the aperture considering the point source case, as described in Hogg et al. (2000). The largest errors in the combined data set are due to the comparatively shallower near-IR data (typically  $\sigma_{HK'} \sim 0.2$  mag).

## 3. Stellar Mass Estimates

The resulting photometric data set covers Un through HK' in the observed frame. The red end of this range corresponds to  $\sim 0.9\mu\text{m}$  in the rest-frame of the highest redshift considered here, and to  $\sim 1.3\mu\text{m}$  for a more typical  $z \sim 0.7$  galaxy in our sample. The blue end corresponds to rest-frame  $\sim 0.18\mu\text{m}$  and  $\sim 0.23\mu\text{m}$ , respectively. Gil de Paz & Madore (2002) have shown that this filter combination is well suited to derive physical properties of galaxies at  $z \sim 0.7$  from broad-band data alone, including star formation timescale, age, metallicity, and stellar mass.

Similarly to the stellar mass estimates method described in BE00, we adopt a grid of evolutionary synthesis models with simple star formation histories (Bruzual & Charlot 2002) and select the most appropriate evolutionary history by error-weighted fitting of the optical and IR photometry. The models have three main parameters: initial mass function (IMF), star formation rate (SFR) history, and metallicity. There are, however, some differences between our method and that described by BE00. Firstly, instead of k-correcting the observed magnitudes for our LCBG sample, we chose to shift all model spectra to the redshift of each of our objects. Redshifted model spectra were convolved with the empirical filter functions corresponding to the actual Un, G, R, F814W, and HK' broadband filters used in the observations to derive the model magnitudes. These

magnitudes were then corrected for extinction assuming not only a range of values for the color excess E(B-V) a la BE00, but also a variety of extinction laws including those derived for the Milky Way (MW; Mathis 1990), Large Magellanic Cloud (LMC; Bouchet et al. 1985), LMC with wavelength-dependent extinction correction (LMC-modified; Mas-Hesse & Kunth, private communication), Small Magellanic Cloud (SMC; Bouchet et al. 1985), and the so-called Calzetti’s law (C94; Calzetti et al. 1994).

Secondly, there is growing evidence that LCBGs, both in the local and distant universe, have a composite stellar population that can be well represented by a young burst superimposed on an older underlying population (Guzmán et al. 1998; Bergvall & Östlin 2001; Östlin et al. 2001; Gruel 2002). We use a composite “underlying+burst” model to fit the observed broadband magnitudes. The burst and underlying components are defined in terms of the assigned star formation rate histories, e.g. instantaneous burst versus constant or exponentially decaying SFR. For simplicity, both populations are assumed to have the same IMF and metallicity. The best fit model is found using a two-step, iterative procedure. Firstly, a single burst model is fitted to the observed Un, G, and R optical bands alone, i.e., the extinction-corrected model magnitudes are compared to the observed magnitudes and the best fit is selected using a simple, weighted, least-squares minimization technique.<sup>7</sup> Weights were scaled with the flux in each band using the limiting magnitudes to provide the reference minimum weight. Since the observed Un, G, and R bands map approximately the rest-frame UV region of the spectrum at the redshifts of our galaxies, light is entirely dominated by the youngest stars in the burst. The fitted model will provide an initial value for the age of the burst. Secondly, we fit a “underlying+burst” model to all observed magnitudes, including F814W and HK’. The burst component is now restricted to vary by less than 10 timesteps (or a factor  $\sim 2$ ) in age from the initial value. Stellar masses are estimated by normalizing the combined “underlying+burst” spectral energy distribution to the observed magnitudes modulo the IMF. Table 1 summarizes the model ingredients.

Over 800 different model combinations were investigated. As shown by Gil de Paz & Madore (2002), the comparison of broad-band photometry with the predictions of evolutionary synthesis models to derive galaxy physical properties yields, in general, highly degenerate results. A first set of “best fit” models were selected on the basis of having the lowest residuals, i.e., the lowest standard deviations for the five differences between model and observed magnitudes.<sup>8</sup> The median

---

<sup>7</sup>No correction for nebular continuum were made to the Un, G, and R magnitudes since its contribution is only significant for burst ages of a few  $10^6$  yr which are ruled out by the H $\beta$  equivalent widths measured for our sample galaxies (Guzmán et al. 1997). The correction for nebular line emission on these broadband magnitudes is estimated to be  $< 10\%$  (Bergvall & Östlin 2002) and were not applied.

<sup>8</sup>During the model fitting procedure, it was found that offsets needed to be applied to the observed magnitudes. We have not been able to identify the source of these offsets. They were derived iteratively as part of the fitting technique. Extensive Montecarlo simulations were performed to ensure that our code could identify and recover artificially introduced zero-point offsets in fake galaxy catalogs that best mimick the properties of our LCBG sample. We are confident that the uncertainty in the derived stellar masses is dominated by model degeneracy and random

residuals of the “best fit” models are less than 0.15 mag. The largest median residuals are  $\sim$ 0.35 mag, which correspond to models that use the MW extinction law with  $E(B-V)=1$ . On this basis alone, we were able to reject the following cases: (i) models with constant SFR for the underlying component; (ii) models with MW and LMC-modified extinction laws; and (iii) models with LMC and SMC laws and  $E(B-V)>0.5$ . The residuals were found to be only slightly dependent on the choice of IMF, metallicity, and star formation timescales. Since there is growing evidence that the IMF in star-forming and starburst regions is universal and consistent with Salpeter’s (Leitherer 1998), we adopt a Salpeter IMF with lower and upper mass cutoffs of 0.08 and  $125 M_{\odot}$ , respectively, for both the burst and underlying components. We also adopt a metallicity  $Z = 0.4Z_{\odot}$ , consistent with the range of metallicities observed in distant LCBGs (Guzmán et al. 1996; Kobulnicki & Zaritski 1999). Finally, we set the star formation timescales to be instantaneous for the burst, and exponential with  $\tau = 1$  Gyr for the underlying component.

The more restrictive choice of parameters reduces significantly the number of “best fit” models. The solutions are, however, still degenerate since various combinations of  $E(B-V)$ , ranging from 0 to 0.5 mag, and extinction laws (LMC, SMC, and C94), all produce a low residuals fit to the data. Since the timescales for the burst and underlying components in the models are now fixed, we find that the dominant source of degeneracy is the age-extinction degeneracy (Gil de Paz & Madore 2002). This is in the sense that an older burst with less dust-extinction may yield as good fit to the data as a younger but more extincted burst. If the burst is assumed to be less than  $10^8$  yrs old, as suggested by the relatively strong  $[\text{OII}]\lambda 3727$  and  $H\beta$  equivalent widths (Guzmán et al. 1997), then we find only one “best-fit” model that fulfills all the conditions described in our analysis. According to this model, LCBGs are consistent with being experiencing, on average, a 9% burst of star formation that is only 13 Myrs old. This young component is superimposed on an older, redder population that is, on average, 2 Gyrs old. These results are qualitatively in good agreement with the burst strength and age estimates based on mass-to-light ratios and color analysis for a different sample of LCBGs (Guzmán et al. 1998). The derived amount of extinction,  $E(B-V)=0.5$  mag, is also in good agreement with the average value measured in starburst galaxies similar to LCBGs (Gil de Paz et al. 2000; Hammer et al. 2001; Rosa-González et al. 2002). We emphasise, however, that the results on the stellar mass measurements are remarkably independent on the final model choice, as it is discussed below.

Figure 1 shows the distribution of stellar masses for our LCBG sample. The median value of the overall distribution is  $5 \times 10^9 M_{\odot}$ . This value is very similar to that derived for nearby LCBGs (Östlin et al. 2001). Note, however, that this value is about  $\sim 10$  times smaller than the average stellar mass in Hammer et al.’s (2001) sample of compact galaxies at intermediate redshifts. This difference is most likely due to the intrinsic higher luminosity of Hammer et al.’s sample, and the fact that these authors adopted a different K-band mass-to-light ratio. The median values for

---

photometric errors, as explained in the text, and not by offset errors, which contribute only 0.1-0.15 dex to the mass estimates.

the HII-like and SB disk-like LCBGs are  $5 \times 10^9 M_{\odot}$  and  $2 \times 10^{10} M_{\odot}$ , respectively. Although non-significant in this small sample, these values suggest that SB disk-like LCBGs tend to be more massive than HII-like LCBGs. The mean value for the subsample of 17 LCBGs with blue luminosities around  $L^*$  (i.e.,  $M_B^* \pm 1$ ) is  $1.8 \pm 1 \times 10^{10} M_{\odot}$ . This value is one order of magnitude lower than the stellar mass expected for a local  $L^*$  galaxy. Assuming  $M_K^* = -25.1$  (for  $H_0 = 50 \text{ km s}^{-1} \text{ Mpc}^{-1}$ ; Mobasher, Sharples & Ellis 1993), and a K-band mass-to-light ratio of  $1 M_{\odot}/L_{K,\odot}$  (Héraudeau & Simien 1997), the estimated stellar mass is  $2 \times 10^{11} M_{\odot}$ . Thus, we conclude that the  $L^*$  CBGs at intermediate redshifts are about 10 times less massive than a typical  $L^*$  galaxy today. This result is in good agreement with previous claims based on virial mass estimates (Koo et al. 1994; Guzmán et al. 1996; Phillips et al. 1997). Our conclusion is not affected by the final choice of the model we adopted here. The median value for the stellar mass estimates derived from the other “best-fit” models differ in a factor  $\sim 2$  from the median value given above. The highest values correspond to models using the C94 extinction law, which yield a median stellar mass of  $1.3 \times 10^{10} M_{\odot}$ . We also note that a Salpeter IMF yields systematically higher masses, although only by  $0.2 \pm 0.05$  dex. The use of a different IMF would strengthen our conclusion. Most interestingly, we find that LCBGs at intermediate redshifts span the same range of stellar masses and stellar mass-to-light ratios as that characteristic of Lyman-break galaxies at redshifts  $z \sim 3$  (Papovich, Dickinson & Ferguson 2001).

Figure 2 shows the comparison of the stellar masses with virial masses derived by Phillips et al (1997). The virial masses used for this figure have been corrected for a systematic underestimate of the galaxy gravitational potential when emission-line velocity widths are used. This effect amounts to a  $\sim 30\%$  increase in observed velocity widths (Guzmán et al 1996; Rix et al 1997; Phillips et al 1997; Pisano et al 2001). No corrections for inclination were made. Rotationally-supported, face-on LCBGs are likely to have virial masses significantly lower than their stellar masses. The  $1-\sigma$  error bars have been calculated by propagating the magnitude errors, the standard deviations of the fit residuals, and the quoted errors in half-light radii and velocity widths. The largest source of uncertainty is associated to the errors in the shallower HK' photometry. The average error in the stellar mass measurements amounts to 0.36 dex (in logM). Excluding the two most uncertain measurements, the average of the estimated errors drop to 0.27 dex, i.e., a factor of  $\sim 2$ . This value is comparable to the median error estimated by BE00 in their error analysis. The average random error for the virial mass measurements is estimated to be 0.18 dex. The median virial-to-stellar mass ratio is 0.39 dex. Thus the stellar mass estimates of LCBGs are, on average,  $\sim 2$  times smaller than the virial mass estimates. This result is also in good agreement with the comparison between stellar masses and dynamical masses made by BE00 and Papovich, Dickinson & Ferguson (2001). The scatter in the virial-to-stellar mass ratio is slightly larger than expected from the error analysis, although the exclusion of the two most deviant points results in 0.54 dex, or a scatter of a factor  $\sim 3$ . No systematic differences in the virial-to-stellar mass ratios are detected between the SB disk-like and HII-like LCBGs. We note, however, that Figure 2 suggests a trend in the sense that the lowest stellar mass LCBGs tend to have the highest virial-to-stellar mass ratios.

#### 4. Conclusions

We have presented a new method for determining robust stellar masses for LCBGs up to redshifts  $z \sim 1.2$ . Our method expands on previous work in the field by including a two-component “burst+underlying” model population fitted to a combination of rest-frame UV, optical and near-IR broad-band photometry in an iterative fashion. Although specifically tailored for starburst galaxies with a composite stellar population, this method can also be used to estimate the stellar masses of the field galaxies in general of known redshift. According to our best-fit model, LCBGs at intermediate redshifts can be described, on average, as starburst systems which are undergoing a 13 Myrs old burst involving 9% of the galaxy mass superimposed on an underlying, older population (2 Gyrs). This model requires a modest amount of extinction ( $E(B-V)=0.5$ ) with a LMC extinction law. We have demonstrated via comparisons and simulations that the stellar masses can be estimated with a precision of  $\log \Delta M_{star} \sim 0.3$  dex, and are not significantly affected by the main assumptions needed to constrain the degeneracy intrinsic to this method. The median stellar mass for LCBGs in our sample is  $5 \times 10^9 M_{\odot}$ , or  $\sim 2.5$  times smaller than previous mass estimates based on the virial theorem using scale lenghts and emission-line velocity widths. The new, independent mass estimates are consistent with previous claims that L\*CBGs at intermediate redshifts are about 10 times less massive than a typical L\* galaxy today.

RG is grateful to the Institut d’Astrophysique de Paris and the Laboratoire d’Astrophysique at the Observatoire Midi-Pyrenees for their hospitality and financial support for this project. RG also acknowledges funding from NASA grants HF01092.01-97A and LTSA NAG5-11635. G.O. acknowledges support from the Swedish Natural Sciences Research Council and the STINT foundation. We thank Roser Pelló for providing k-corrections used for an independent test of the quality of the photometric data, and Jean Michel Desert for helping in the crosscorrelation of the various catalogs.

## 5. References

Alonso-Herrero A., Aragón-Salamanca A., Zamorano J. & Rego M. 1996, MNRAS, 278, 417

Aragón-Salamanca A., Ellis R.S., Couch W.J. & Carter D. 1993, MNRAS, 262, 794

Barger A.J., Cowie L.L., Trentham N., Fulton E., Hu E.M., Songaila A. & Hall D. 1999, AJ, 117, 102

Bergvall N. & Östlin G. 2002, A&A 390, 891

Bouchet et al. 1985, A&A, 149, 330

Brinchmann J. & Ellis R.S. 2000, ApJL, 536, 77

Bruzual G. & Charlot S. 2002, in prep.

Calzetti et al., 1994, ApJ 429, 582

Charlot S. 1998, in Benvenuti P. et al, eds., AIP Conf. Proceedings Vol. 408, The Ultraviolet Universe at Low and High Redshift: Probing the Progress of Galaxy Evolution. American Institute of Physics, New York, p. 403

Gil de Paz A., Aragón-Salamanca A., Gallego J., Alonso-Herrero A., Zamorano J. & Kauffmann G. 2000, MNRAS, 316, 357

Gil de Paz A. & Madore B.F. 2002, AJ, 123, 1864

Gruel N. 2002, Ph.D. thesis, Observatoire de Paris

Guzmán, R., Koo, D. C., Faber, S. M., Illingworth, G. D., Takamiya, M., Kron, R., & Bershady, M. A. 1996, ApJ, 460, L5

Guzmán R., Gallego J., Koo D. C., Phillips A. C., Lowenthal J. D., Faber S. M., Illingworth G. D. & Vogt N. P. 1997, ApJ, 489, 559

Guzmán R., Koo D. C., Jangren, A., Bershady M., Faber S. M. & Illingworth G. D., 1998, ApJ, 495, L13

Hammer, F., Gruel, N., Thuan, T. X., Flores, H., & Infante, L., 2001, ApJ, 550, 570

Héraudeau P. & Simien F. 1997, A&A, 326, 897

Hogg, D.W., Pahre M.A., Adelberger K.L., Blandford R., Cohen J.G., Gautier T.N., Jarrett T., Neugebauer G. & Steidel C.S. 2000, ApJS, 127, 1

Kobulnicky H. D., & Zaritsky D. 1999, ApJ, 511, 118

Koo, D. C., Bershady, M. A., Wirth, G. D., Stanford, S. A., & Majewski, S. R. 1994, ApJL, 427, L9

Koo, D. C. Guzmán, R., Faber, S. M., Illingworth, G. D., Bershady, M. A., Kron, R., & Takamiya, M. 1995, ApJ, 440, L49

Leitherer 1998, in Gilmore G., & Howell D. eds., 38th Herstmonceux Conference, The Stellar Initial Mass Function. ASP Conference Series, Vol. 142, p.61

Leitherer et al. 1999, ApJS, 123, 3

Mallén-Ornelas, G., Lilly, S. J., Crampton D., & Schade D. 1999, ApJ, 518, 83

Mathis 1990, ARA&A, 38

Mobasher B., Sharples R.M. & Ellis R.S. 1993, MNRAS, 263, 560

Östlin G., Amram P., Bergvall N., Masegosa J., Boulesteix J. & Márquez I. 2001, A&A 374, 800

Papovich C., Dickinson M. & Ferguson, H.P. 2001, ApJ, 559, 620

Pérez-González P.G., Gil de Paz A., Zamorano J., Gallego J., Alonso-Herrero A. & Aragón-Salamanca A. 2003a, MNRAS, 338, 508

Pérez-González P.G., Gil de Paz A., Zamorano J., Gallego J., Alonso-Herrero A. & Aragón-Salamanca A. 2003b, MNRAS, 338, 525

Phillips A. C., Guzmán R., Gallego J., Koo D. C., Lowenthal J. D., Vogt N. P., Faber S. M. & Illingworth G. D. 1997, ApJ, 489, 543

Pisano D.J., Kobulnicky H. D., Guzmán R., Gallego J. & Bershady, M. A. 2001, AJ, 122, 1194

Rix H.W. & Rieke M.J. 1993, ApJ, 418, 123

Rix H.W., Guhathakurta P., Colles M. & Ing K. 1997, MNRAS, 285, 779

Rosa-González D., Terlevich E. & Terlevich R. 2002, MNRAS, 332, 283

Table 1. Grid of Model Spectral Energy Distributions

| Parameter         | Range   |
|-------------------|---|
| Age.....          | $10^6$ to $2 \times 10^{10}$ yr in steps of 0.1 in log yr |
| SFR (burst) ..... | Instantaneous and $\tau=1.0$ Gyr                          |
| SFR (underlying)  | $\tau=1.0$ Gyr and constant                               |
| IMF.....          | Salpeter, Kennicutt                                       |
| Metallicity ..... | 0.4 $Z_{\odot}$ , and $Z_{\odot}$                         |
| E(B-V).....       | 0.0, 0.25, 0.5, 1.0 mag                                   |
| Ext. Law .....    | MW, LMC, LMC-modified, SMC, C94                           |

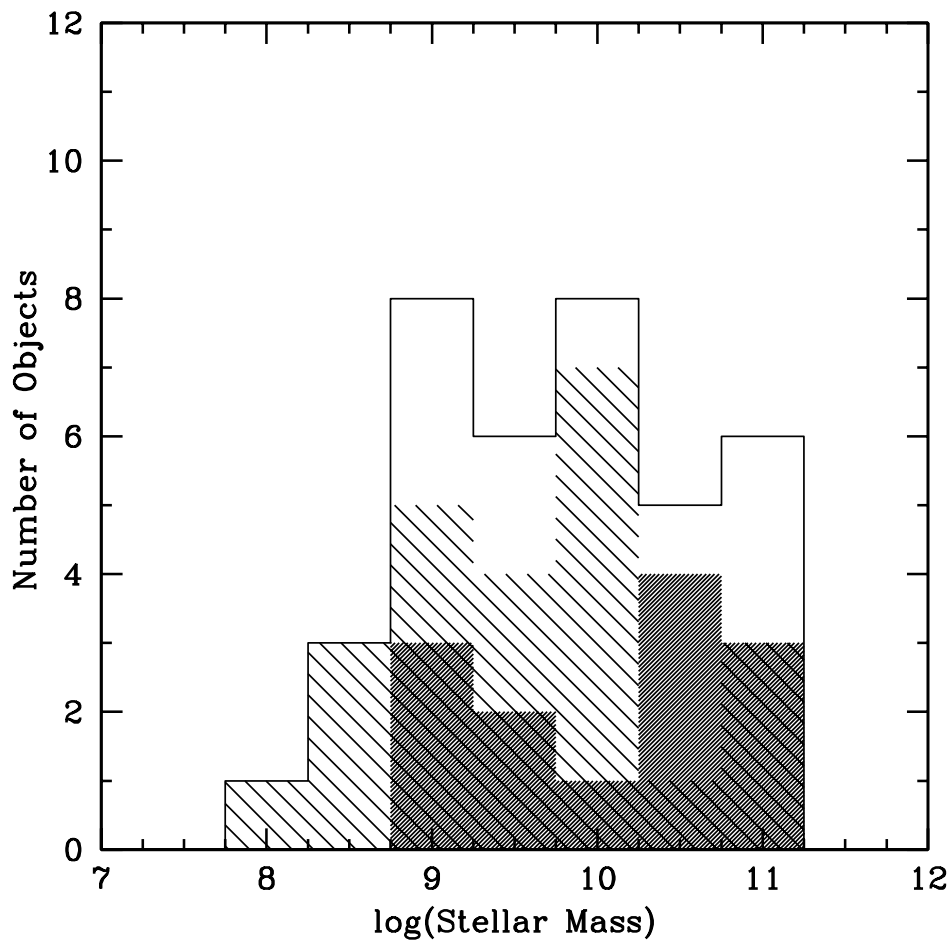


Fig. 1.— Histogram of stellar masses for our sample of LCBGs at intermediate redshift. Solid line: distribution of stellar masses for the whole sample. Grey histogram: distribution of stellar masses for SB disk-like LCBGs. Shaded histogram: distribution of stellar masses for HII-like LCBGs.

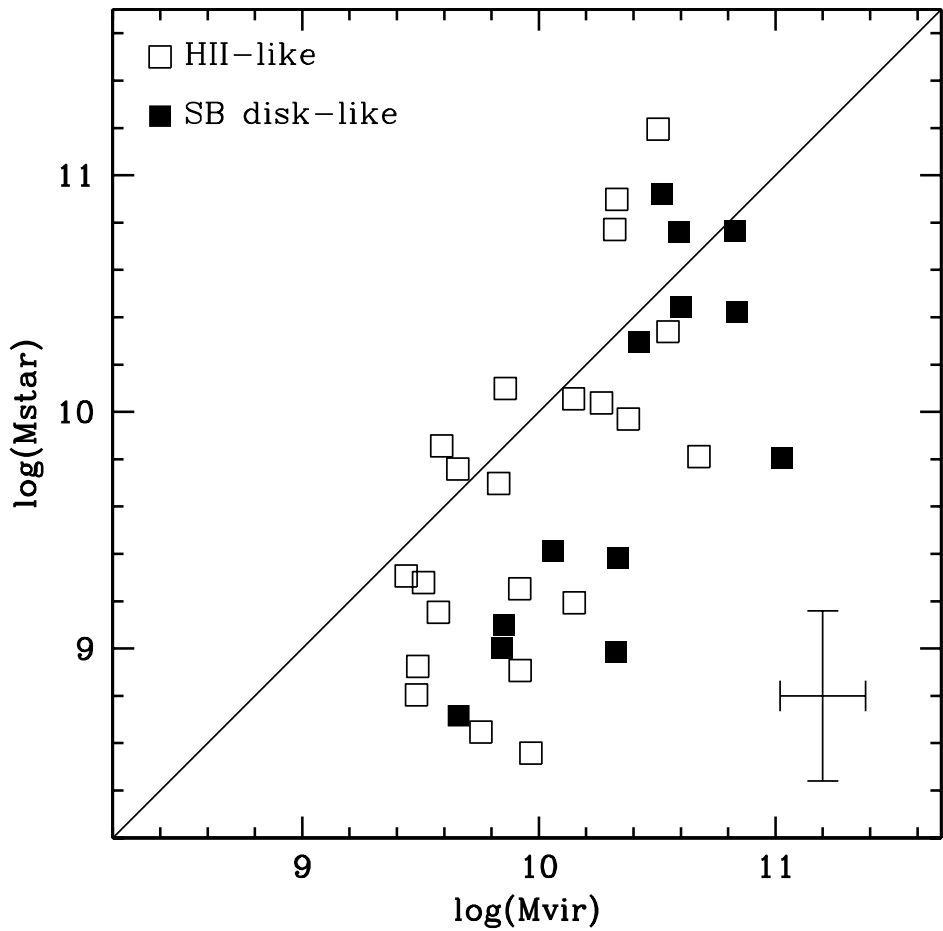


Fig. 2.— The virial mass versus stellar mass for LCBGs in our sample in  $\log(M_\odot)$  units. Open squares: HII-like LCBGs; solid squares: SB disk-like LCBGs. Error bars correspond to average 1- $\sigma$  errors.